



# Fixed Capacitor Magnetically Controlled Reactor Reliability Modeling Considering Environmental Conditions

Morteza Haghshenas\*, Rahmat-Allah Hooshmand

Department of Electrical Engineering, Faculty of Engineering, University of Isfahan, Isfahan, Iran, Haghshenas.Research@gmail.com

## Abstract

The fixed capacitor-magnetically controlled reactor (FC-MCR) is a type of static var compensator (SVC) that can greatly contribute to the availability and stability of power systems. This paper proposes a comprehensive reliability model for the FC-MCR using the Markov process approach. The modeling process adheres to actual operational principles and divides the MCR structure into two sections: electro-magnetic section and core magnetization section. Subsequently, the Markov models proposed for these sections are integrated with the Markov model of the fixed capacitor bank to derive the FC-MCR reliability model. Recognizing the impact of environmental conditions on electrical equipment failure rates, the proposed reliability model takes into account temperature variations and assesses their influence on the probabilities of the FC-MCR operating state. By examining the simulation results and conducting sensitivity analysis, it was found that the availability of the FC-MCR is influenced by various components and environmental conditions, which necessitates different reliability enhancement measures. Moreover, a comparison between the reliability indices of the FC-MCR and its counterpart (FC-TCR) in diverse environmental conditions revealed that the FC-MCR is less affected by temperature variations compared to the FC-TCR.

Keywords: Fixed Capacitor Magnetically Controlled Reactor, Temperature effect on Reliability indices, MIL-217F Standard.

Article history: Received 2024/01/02; Revised 2024/02/05; Accepted 2024/02/10. Article Type: Research paper

© 2024 IAUCTB-IJSEE Science. All rights reserved

<https://doi.org/10.82234/ijsee.2024.1074788>

## 1. Introduction

### A) Fixed Capacitor Magnetically Controlled Reactor (FC-MCR)

By developing the power systems and raising issues such as privatization and deregulation in the electricity industry, paying attention to the reactive power problems and a need for compensators with high flexibility and reliability are necessary. In the meantime, Static var compensator (SVC) as one of the most conventional reactive power sources in power systems, plays an important role in voltage stability and control, loss reduction, and power quality enhancement [1]. The fixed capacitor-thyristor controlled reactors (FC-TCR) and thyristor switched capacitor thyristor controlled reactors (TSC-TCR) are two common types of SVCs used in power systems. Fixed capacitor magnetically controlled reactor (FC-MCR) is a type of SVCs that due to its advantages has recently been widely used in power systems [2].

MCR is a type of flexible AC transmission systems since 1990; it has been used for voltage

stability and reactive power control in power systems. The utilization of MCR alongside fixed capacitor banks creates a new type of SVC with the advantages of continuously adjustable capacity, low harmonic, and excellent control characteristics that can be connected to the power system with no need for an interface transformer [2]. As shown in Fig. 1, the MCR structure consists of two electromagnetic (EMS) and core magnetization sections (CMS). The EMS including control, compensation, and HV windings (wd), windings cooling system (WCS), tank and oil (T&O), iron core, HV bushings (bsh), and CMS including a thyristor-controlled rectifier (Rec.), thyristors cooling system (ThCS), and MCR control system (MCRCS). In this configuration, the reactive power generated by FC is fixed and the reactive power absorption capacity is controlled by MCR through magnetizing the iron core [3]. Connecting the HV windings to the power system creates an AC flux in the iron core, which induces the AC voltage in the compensator winding, and finally, feeds the DC link of the rectifier. By controlling the thyristors firing angle of the rectifier,

the controllable voltage of  $V_{DC}$  is generated and applied to the MCR control winding. Applying  $V_{DC}$

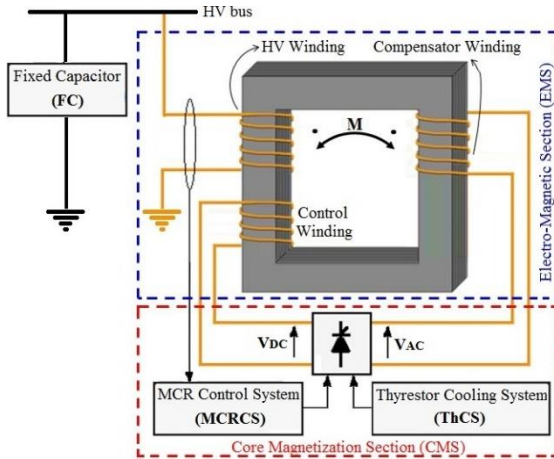


Fig. 1. General Structure of FC-MCR Type of SVC.

to the control winding creates a bias in the magnetic core, followed by the change of the core operating point and its saturation. In the saturation region, a slight variation in the voltage can lead to extensive variation in the current. Hence, by creating a bias in the iron core, the value of reactance can be changed from the HV winding point of view [4].

The core bias circuit has a slight power compared to MCR rated power. This causes the thyristors used in the MCRCS to be subjected to slight voltage and current compared to the thyristor valves used in the TCR structure and limits the need for the ThCS operation. Ultimately, the reduction in the heat generated in thyristors reduces the sensitivity of MCR to rectifier parameters and its cooling system. However, in the TCR-based SVCs, flowing total reactor current through the thyristor valve leads to high switching losses followed by an intense temperature increase in the thyristor valves. Furthermore, the direct connection of MCR to the HV network and the lack of a need for an interface transformer can have a significant effect on increasing availability of the MCR-based SVCs.

### B) Literature Review

Since, in many cases, reactive power variations in transmission lines are more than active power variations [5], SVCs can have a significant effect on the availability and stability of power systems. Hence, it is necessary to consider the role of these compensators and the factors such as environmental conditions affecting their performance in power system reliability evaluation [6]. Reliability is defined as the probability that a system, or service will perform its intended function adequately for a specified period, or will operate in a defined environment without failure [7-8]. Generally, reliability evaluation methods can be divided into two categories, i.e. the analytical methods and Monte-Carlo simulation techniques [9-10]. In

analytical methods based on the states enumeration, all possible states are examined one by one and each state is separately analyzed. In Monte-Carlo simulation methods based on the random behavior of the system, the reliability indices are estimated by actual process simulation [10]. A Markov chain is a stochastic model that uses mathematics to predict the probability of a sequence of events occurring based on the most recent event. The defining characteristic of a Markov chain is that no matter how the process arrived at its present state, the possible future states are fixed. In other words, the probability of transitioning to any particular state is dependent solely on the current state and time elapsed [7].

In this regard, in [6] and [11-15] some new indices are presented for the reliability evaluation of a power system in conditions where reactive power sources are incapable, and the network points needed for reactive power compensation are specified based on these indices. In [13], the effect of using a unified power flow controller (UPFC) on power system reliability indices has been evaluated, and shown that the utilization of this controller will significantly decrease the expected energy not served (EENS). In [14], the effect of power factor correction capacitors on the electrical distribution system reliability has been evaluated; calculating the reliability indices with and without the presence of capacitor banks has shown that these sources have a significant effect on the reliability enhancement of the electrical distribution system. In [15], a two-state reliability model is presented by combining the Markov process and Monte-Carlo simulation methods for the FC-TCR. In this method, Monte-Carlo simulation was used to extract the reliability parameters, while the Markov process was used to calculate the reliability indices. In the modeling process presented in [15], the effect of the control system has not been considered as the most sensitive component of SVC, and derated states have been ignored. In this regard, a three-state reliability model for the FC-TCR type of SVC is presented in [16], where in addition to in-service and out-of-service states, derated states are also considered. The results presented in [16] have shown that the TCR will have the greatest effect on SVC availability due to the high temperature in the thyristor valve.

In the FC-TCR type of SVC, the TCR is responsible for the continuous control of reactive power by controlling the effective current amplitude flowing toward the reactor. In the FC-MCR type of SVC, reactive power absorption capacity is controlled by the magnetization of the iron core. In this compensator, by removing the thyristor valve from the reactor structure, direct connection to a high voltage (HV) network is possible [2]. Previously, magnetically and thyristor-controlled reactors have been compared in transient behaviors and harmonic points of view [17-18]. The

results presented in [17] show that with no need for harmonic filters, MCR can control reactive power and system voltage with an output of less than 2% of the total harmonic distortion. In [18], it has been shown that although MCR-based SVCs have slower response rates than TCR-based SVCs, they can play a more prominent role in power system transient stability enhancement. However, no model has been provided for evaluating the reliability of MCR and MCR-based SVCs in the literature so far.

### C) The Proposed Modeling Approach

In this paper, a comprehensive reliability model has been proposed based on the Markov process approach for the FC-MCR. In the proposed approach that performed according to real operation principles, the MCR structure is divided into two electro-magnetic and core magnetization sections and next, the extracted reliability models for them is combined with the reliability model of the FC. The proposed process for reliability modeling takes into account the impact of environmental conditions on key parameters, such as the failure rates. The proposed reliability model is a general model that can be applied to FC-MCR in the power system, irrespective of its capacity. This paper is organized as follows: Section 2 is dedicated to the reliability modeling of FC-MCR and its components. The effect of operating temperature on FC-MCR components failure rate has been investigated in section 3. The simulation results are presented in Section 4. Finally, this paper is concluded in Section 5 and further work have been provided.

## 2. The Proposed Reliability Model for FC-MCR

In this section, EMS and CMS reliability models have been extracted based on the relationship of the components using the Markov process technique and by combining them with the FC model; the final reliability model is determined for the FC-MCR. The main steps in deriving the FC-MCR reliability model are as follows:

**Step 1:** Determining the Rec, ThCS and MCRCS Markov models according to the failure modes and their combination (based on the relationship of components) to derive the core magnetization section reliability model.

**Step 2:** Determining the Markov models of MCR internal components including windings, core, oil and oil tank according to the failure modes and their combination to derive the subsystem 1 Markov model in the electromagnetic section.

**Step 3:** Determining the Markov models of MCR external components including bushings and MCR control system according to the failure modes and their combination to derive the subsystem 2 Markov model in the electromagnetic section.

**Step 4:** Combining the Markov model of subsystems 1 and 2 to derive the electromagnetic section Markov model.

**Step 5:** Combining the Markov model of core magnetization and electromagnetic sections to derive the MCR Markov model.

**Step 6:** Determining the Markov model of fixed capacitor bank according to its failure modes and combining the Markov model of FC and MCR to derive the FC-MCR reliability model.

**Step 7:** Applying the impact of environmental conditions on the performance of FC-MCR components according to the MIL-217F standard [22] and determining reliability value in various operational modes and environmental scenarios.

The modeling process and calculated parameters in each step are presented in Fig. 2, and the details are presented below. In this regard, it is assumed that all of the components are non-redundant and have two operation states in service (UP) and out of service (DN), except for the reactor windings that can have the derated (DR) state.

### A) The Proposed Reliability Model for MCR Core Magnetization Section

As mentioned in Section 1.2, CMS consists of Rec., ThCS, and MCRCS, so if one of the components fails, all the CMS and then MCR will be removed from the service. This means CMS components are in series from a reliability point of view. Accordingly, the equivalent failure and repair rates for CMS are calculated by (1) and (2), and the Markov model shown in Fig. 3 is determined for this part of the reactor.

$$\lambda_{CMS} = \lambda_{MCRCS} + \lambda_{rec} + \lambda_{ThCS} \quad (1)$$

$$\mu_{CMS} = (\lambda_{MCRCS} + \lambda_{rec} + \lambda_{ThCS}) \times \left( \frac{\lambda_{MCRCS}}{\mu_{MCRCS}} + \frac{\lambda_{rec}}{\mu_{rec}} + \frac{\lambda_{ThCS}}{\mu_{ThCS}} \right)^{-1} \quad (2)$$

### B) The proposed Reliability Model for the MCR Electro-Magnetic Section

In this section, to avoid the Markov Model complexity and equations governing it, the EMS is separately modeled in the form of two subsystems 1 (SS1) and 2 (SS2), and by combining their models based on the frequency/duration technique [9], the EMS final Markov model is determined. In this classification, the SS1 contains active components such as windings, iron core, insulation fluid, and SS2 contains passive components such as bushings and WCS.



Fig. 2. Proposed model for core magnetization section (CMS).

**Reliability Modeling of Subsystem 1:** In this subsystem, MCR derated or out-of-service states can occur due to the windings failure. According to SVC loading conditions, by reducing the compensation load to about 20-50 percent of rated power in this case, the MCR can remain in service [19-20]. In this paper, the state in which SVC failure leads to limiting the available capacity for reactive power compensation is called the derated state. Accordingly, the reliability model of MCR windings includes three states of in-service (UP), derated (DR), and out-of-service (DN) as presented in Fig. 4(a). For SS1 other components reliability modeling, it is assumed that the iron core has two states, i.e. UP and DN, and that both oil and its tank are considered as one component. Here, these components will be modeled in the form of a set called CTO. Since the failure of each of these components can fail SS1, the equivalent failure and repair rates for CTO are calculated by (3) and (4), and the two-state Markov model shown in Fig. 4(b) is determined for this part of the SS1.

After determining the windings and CTO set Markov model, we can achieve the reliability model of SS1 by combining the models presented in Figs. 4(a) and 4(b). The final Markov model of SS1 is

shown in Fig. 4(c). A remarkable point in Fig. 4(c) is the transfer from state C to D. In this model, when the windings are in a derated state (state C), failure in each of the other components causes the SS1 to be removed from service (state D). In this situation, since the SS1 is completely out-of-service, the repairing actions on the windings are similar to the state in which windings have removed this subsystem from the service. The SS1 Markov model can be reduced by using (5) – (15) as shown in Fig. 4(d). In this model, States 1, 2, and 3 represent the full, zero, and derated capacity of SS1, respectively.

$$\lambda_{CTO} = \lambda_{Core} + \lambda_{T \& O} \quad (3)$$

$$\mu_{CTO} = (\lambda_{Core} + \lambda_{T \& O}) \left( \frac{\lambda_{core}}{\mu_{core}} + \frac{\lambda_{T \& O}}{\mu_{T \& O}} \right)^{-1} \quad (4)$$

$$P_1 = P_A \quad (5)$$

$$P_2 = P_B + P_E + P_D \quad (6)$$

$$P_3 = P_C \quad (7)$$

Where  $P_1$ ,  $P_2$  and  $P_3$  are the probabilities of UP, DN, and DR states for the simplified Markov model of SS1, respectively. Accordingly, in Fig. 4(d), the transfer frequency between states can be calculated by (8) – (11) and its equivalent repair and failure rates by (12) – (15).

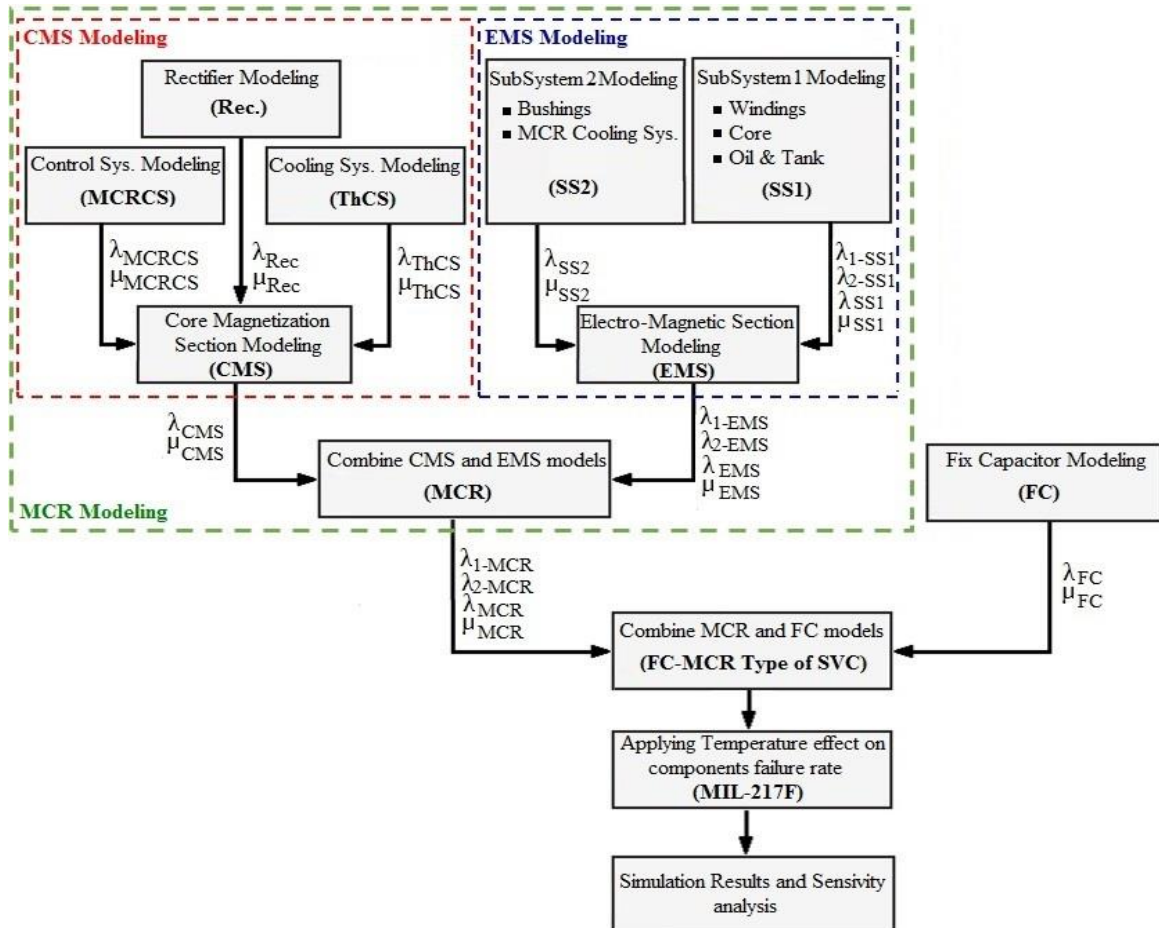


Fig. 3. The FC-MCR Reliability Modeling Process.

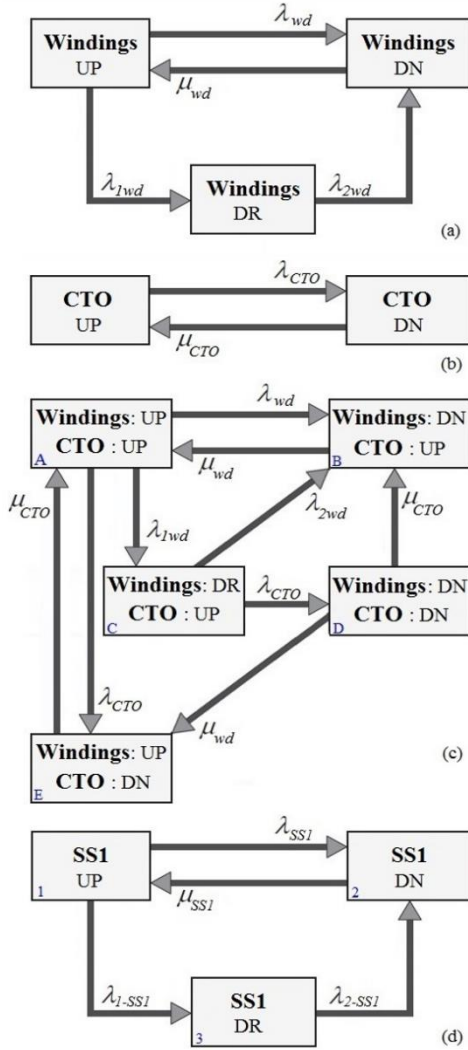


Fig. 4. Three-state Markov model for windings (a), Two-state Markov model for CTO Set (b), Proposed Markov model for SS1 (c), Reduced Markov model for SS1 (d).

$$f_{12} = f_{AB} + f_{AE} = (\lambda_{wd} + \lambda_{CTO})P_A \quad (8)$$

$$f_{13} = f_{AC} = \lambda_{1wd} \cdot P_A \quad (9)$$

$$f_{21} = f_{BA} + f_{EA} = \mu_{wd} \cdot P_B + \mu_{CTO} \cdot P_E \quad (10)$$

$$f_{32} = f_{CB} + f_{CD} = (\lambda_{2wd} + \lambda_{CTO})P_C \quad (11)$$

$$\lambda_{SS1} = \frac{f_{12}}{P_1} = \lambda_{wd} + \lambda_{CTO} \quad (12)$$

$$\lambda_{2-SS1} = \frac{f_{32}}{P_3} = \lambda_{2wd} + \lambda_{CTO} \quad (13)$$

$$\lambda_{1-SS1} = \frac{f_{13}}{P_1} = \lambda_{1wd} \quad (14)$$

$$\mu_{SS1} = \frac{f_{21}}{P_2} = \frac{\mu_{wd}P_B + \mu_{CTO}P_E}{P_B + P_E + P_D} \quad (15)$$

**Reliability Modeling of Subsystem2:** Since the bushings failure results in an insulation breakdown,

in the reliability modeling of SS2, two states are considered for HV bushings, UP and DN. In addition, it is assumed that the MCR used the natural circulation of oil and the natural circulation of air to cooling the windings. Accordingly, the WCS can be modeled by two UP and DN states. Therefore, using the forced cooling methods for reactor windings can also add a derated state to its Markov model. Because the operation of SS2 depends on both its components being healthy, the two-state Markov model shown in Fig. 5 is proposed for this subsystem by using the following equations.

$$\lambda_{SS2} = \lambda_{WCS} + \lambda_{Bsh} \quad (16)$$

$$\mu_{SS2} = (\lambda_{WCS} + \lambda_{Bsh}) \left( \frac{\lambda_{WCS}}{\mu_{WCS}} + \frac{\lambda_{Bsh}}{\mu_{Bsh}} \right)^{-1} \quad (17)$$

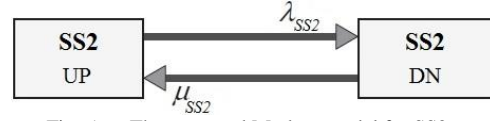


Fig. 5. The proposed Markov model for SS2.

**Combining the Subsystems 1 and 2:** In this section, the proposed Markov models for SS1 and SS2 in the EMS are combined and the result is presented in Fig. 6(a). Here, similar to Section 3.2.1, by merging the corresponding DN states based on the frequency/duration technique concepts, the EMS reduced Markov model can be extracted by using (18) – (21) as shown in Fig. 6(b). It is obvious that when using the common equations to simplify the Markov model in Fig. 6(a), the numerical values of the probabilities and frequencies between the system states will be different from those calculated in Section 2.2.1 due to the difference in the base Markov model parameters.

$$\lambda_{EMS} = \lambda_{SS1} + \lambda_{SS2} \quad (18)$$

$$\lambda_{2EMS} = \lambda_{2-SS1} + \lambda_{SS2} \quad (19)$$

$$\lambda_{1EMS} = \frac{\lambda_{1-SS1}P_A}{P_A} = \lambda_{1-SS1} \quad (20)$$

$$\mu_{EMS} = \frac{\mu_{1-SS1}P_B + \mu_{SS2}P_E}{P_B + P_E + P_D} \quad (21)$$

#### A) Combining EMS and CMS Markov models

In this section, to reliability modeling of MCR, the Markov models presented in Figs. 3 and 6(b) are combined and the result is presented in Fig. 7(a). In this regard, it may be claimed that when EMS operates in derated state, failure in CMS causes the MCR to be completely removed from service. In this condition, because the MCR is out of service, the repairing actions on the EMS is similar to the state

in which the EMS have been removed MCR from service. By merging the corresponding DN states in Fig. 7(a), the MCR Markov model can be reduced by using (22) – (25) as shown in Fig. 7(b). In this model, States 1, 2, and 3 represent the full, zero, and derated capacity of MCR, respectively.

$$\lambda_{MCR} = \frac{\lambda_{EMS} P_A + \lambda_{CMS} P_A}{P_A} = \lambda_{EMS} + \lambda_{CMS} \quad (22)$$

$$\lambda_{2-MCR} = \frac{\lambda_{2EMS} P_C + \lambda_{CMS} P_C}{P_C} = \lambda_{2EMS} + \lambda_{CMS} \quad (23)$$

$$\lambda_{1-MCR} = \frac{\lambda_{1EMS} P_A}{P_A} = \lambda_{1EMS} \quad (24)$$

$$\mu_{MCR} = \frac{\mu_{EMS} P_B + \mu_{CMS} P_E}{P_B + P_E + P_D} \quad (25)$$

A) Combining FC and MCR Markov models

In this section, to determine the final Markov model for the FC-MCR, the MCR and FC Markov models are combined. In this regard, for a fixed capacitor whose type is usually AC with mica insulation, two UP and DN states are considered. Accordingly, a combination of the FC two-state and MCR three-state Markov models is shown in Fig. 8. In this model, state A indicates the condition where two components are healthy and SVC can have a reactive power exchange with the network in the nominal range. Failure occurring in FC converts SVC into a variable reactor and eliminates the ability to inject reactive power into the network. These conditions are modeled by states D and E in the Markov representation of Fig. 8 so that the reactive power absorption capability from the network in state D is equal to that of the MCR rated capacity and in state E, it is about 50-80 percent of this value because of derated state of the reactor windings. This fact is visible in SVC V-I characteristics in Fig. 9 [21]. Similarly, the failures resulting in the MCR derated state can reduce the reactive power absorption capacity from the network and limit the SVC performance to compensate for possible over-voltages. Therefore, the failures that cause the MCR to be removed from service will convert SVC into a fixed capacitor bank, in which there will be no reactive power absorption capability in addition to the lack of continuous control of reactive power exchanged with the network. These conditions are modeled in FC-MCR Markov representation with states B and C, respectively. Here, each of states D, C, B, and E in Fig. 8 represents a derated state for FC-MCR and their occurrence can lead to the limitation of reactive power compensation. The FC failure before repairing the MCR or MCR failure before repairing

the FC can lead to the SVC being completely removed from service (state F).

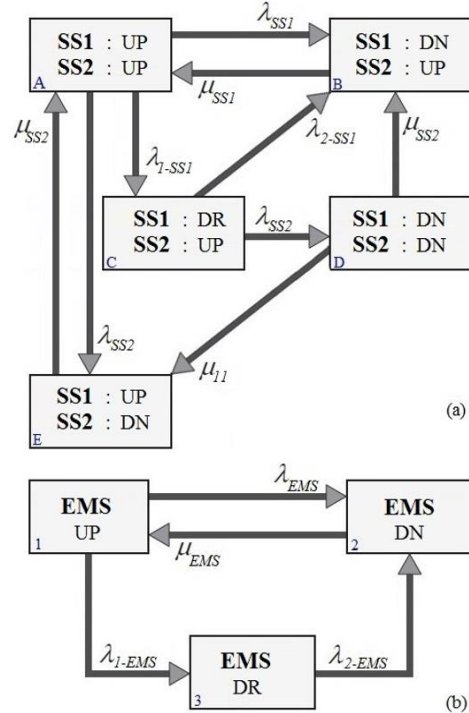


Fig. 6. Proposed Markov model for EMS (a), reduced Markov model for EMS (b).

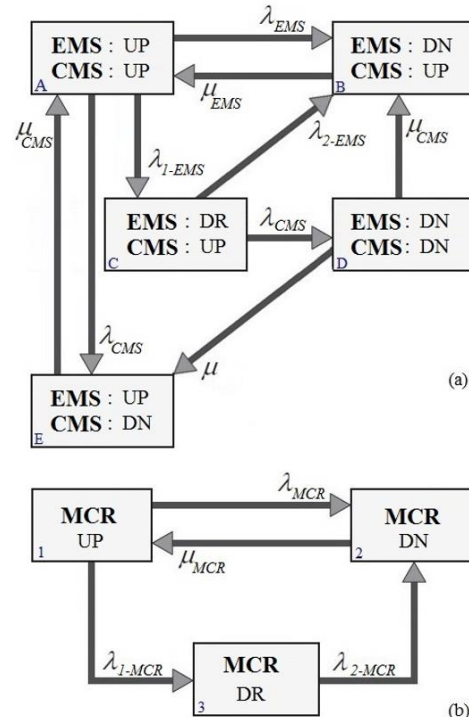


Fig. 7. Proposed Markov model for MCR (a), reduced Markov model for MCR (b).

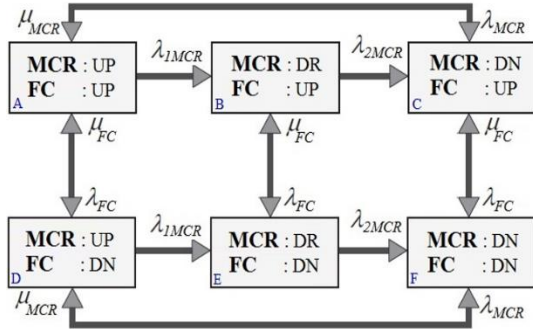


Fig. 8. The proposed Markov model for the FC-MCR.

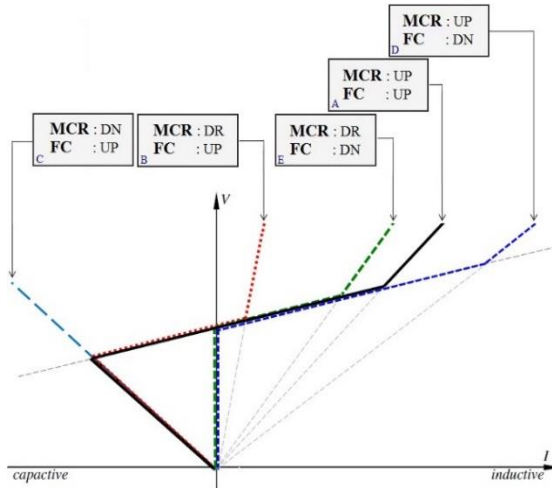


Fig. 9. The FC-MCR type of the SVC V-I characteristic [16].

### 3. Effect of Environmental Conditions on FC-MCR Reliability Indices

Since ambient temperature varies considerably in different areas and operating conditions, thermal management can be one of the important factors affecting the electrical equipment failure rate. In this regard, the effect of environmental conditions on the reliability indices of a power transformer has been evaluated in [19] based on the MIL-217F standard [22] and the results have shown that temperature rise can significantly reduce the availability of the system. Several thermal models have been presented in the literature to represent the effect of temperature on the electronic component failure rate [23-24]. Some literature has examined the component failure rate change of power electronics converters based on the MIL-217F standard [24]. However, the effect of temperature and operating conditions on the reliability of reactive power compensator has not been taken into account so far. Hence, in this section, the effect of temperature variations will be evaluated on the FC-MCR main components failure rate.

#### B) Failure Rate of TCR

Based on the MIL-217F standard, the failure rate of each thyristor in the rectifier structure can be represented as a function of the operating

conditions, environmental factors, and construction quality calculated as follows:

$$\lambda_{Th} = \lambda_{b-Th} \cdot \pi_{T-Th} \cdot \pi_Q \cdot \pi_E \cdot \pi_S \frac{\text{failure}}{10^6 \text{ hr}} \quad (26)$$

The process of calculating the coefficients is presented in [19] and [22], and since the contents of this section are concentrated around the effect of temperature on the component failure rate, the numerical values of these factors are all considered to be one. In addition,  $\pi_{T-Th}$  is called the temperature factor in this section and can be calculated as follows:

$$\pi_{T-Th} = \exp \left\{ \begin{array}{l} 1925 \times \left( \frac{1}{298} \right) \\ - \frac{1}{(T_A + \theta_{ja} \cdot P_{loss}) - 273} \end{array} \right\} \quad (27)$$

#### C) Failure Rate of MCR Windings

MCR windings are affected by the combination of electrical, thermal, and mechanical stresses throughout their lifetime. To represent the effect of temperature on windings failure rate, in addition to the operating temperature, the temperature variation rate relative to normal conditions (27°C) should be considered [22]. Hence, the failure rate of reactor windings under various temperature conditions can be calculated as a function of base failure rate, and base failure rate can be calculated as a function of temperature variations and winding parameters as follows:

$$\lambda_{winding} = \lambda_{b-wd} \cdot \pi_Q \cdot \pi_E \cdot \pi_S \frac{\text{failure}}{10^6 \text{ hr}} \quad (28)$$

$$\lambda_{b-wd} = 0.0015 \times \left( \frac{T_{HS} + 273}{477} \right)^{8.4} \quad (29)$$

$$T_{HS} = T_A + 1.1 \Delta T \quad ^\circ C \quad (30)$$

Equations (28) – (30) are presented for the reactor with the assumption of an H insulation class (180°C max operating temperature). Based on the Markov model proposed for MCR, Equations (28) – (30) can be used to represent the effect of temperature on the failure rate of windings from state UP to DR, state DR to DN, and state UP to DN.

#### D) Failure Rate of ThCS

The ThCS is usually composed of a heat exchanger, interconnecting pipes, and a circulation pump that performs heat transfer by circulating water inside the heat sinks. Since the highest failure probability in ThCS is related to the circulation pump (including an induction motor), in this section, the effect of temperature is only examined for the failure rate of this equipment. Temperature variations in addition to their effect on the failure rate of electrical parts such as windings, can also lead to a change in the failure rate of mechanical

parts such as bearings [22]. Hence, the circulation pump failure rate is calculated as follows:

$$\lambda_{ThCS} = \lambda_{b-ThCS} \cdot \pi_Q \cdot \pi_E \cdot \pi_S \cdot \frac{\text{failure}}{10^6 \text{ hr}} \quad (31)$$

Where:

$$\lambda_{b-ThCS} = \left[ \frac{t^2}{\alpha_B^3} + \frac{1}{\alpha_w} \right] \times 10^6 \quad (32)$$

$$\alpha_w = 10^{\left( \frac{2357}{T_A + 273} - 1.83 \right)} \quad (33)$$

$$\alpha_B = \left[ 10^{\left( \frac{2.534 - \frac{2357}{T_A + 273}}{20 - \frac{4500}{T_A + 273}} \right)} + \frac{1}{10^{\left( \frac{20 - \frac{4500}{T_A + 273}}{20 - \frac{4500}{T_A + 273}} \right)} + 300} \right]^{-1} \quad (34)$$

#### E) Failure Rate of MCRCS

Considering the MCRCS main components, hardware and software relationship requires detailed information about the control system components for representing the effect of temperature. Here, due to the lack of access to credible reliability parameters of the control system components, the most sensitive component to temperature variation (local microprocessor) is considered as a MCRCS model, and the effect of temperature on its failure rate is represented as follows:

$$\lambda_{MCRCS} = \lambda_{b-MCRCS} \times \pi_{T-MCRCS} \cdot \pi_Q \cdot \pi_E \cdot \pi_S \cdot \frac{\text{failure}}{10^6 \text{ hr}} \quad (35)$$

Where:

$$\pi_{T-MCRCS} = \exp \left\{ \frac{0.235}{8.617 \times 10^{-5}} \times \left( \frac{1}{298} - \frac{1}{T_A - 273} \right) \right\} \quad (36)$$

#### F) Failure Rate of Insulation Fluid and HV Bushings

Every 10°C rise in temperature relative to a base value of 90°C can result in insulation aging and halving the useful life of the insulation fluid and bushings [20]. In this case, the calculation of failure rates for oil and bushings under various temperature conditions are similar to those of the previous sections; the numerical value of the temperature factor for the expression of the effect of temperatures above 90°C on these components failure rate is calculated as follows:

$$\pi_{T-Bsh} = \frac{\lambda_2}{\lambda_1} = e^{B_T \left( \frac{1}{T_1} - \frac{1}{T_2} \right)} \quad (37)$$

Where  $B_T$  can be determined using the half-life rule for each 10°C rise of insulation temperature above 90°C by the following equation.

$$B_T = \frac{\text{Ln}(1/2)}{\left( \frac{1}{T_1} \right) - \left( \frac{1}{T_2} \right)} \quad (38)$$

#### G) Failure Rate of Fix Capacitors

Fixed capacitor banks used in the SVC structure are affected by voltage fluctuations, transient waves, and operating temperatures throughout their lifetime [22]. Hence, in addition to increasing the FC failure rate, temperature variations can also change their capacity. Accordingly, depending on their type, changes in the FC failure rate can be specified as a function of operating conditions; their temperature factor is calculated as follows:

$$\pi_{T-FC} = \exp \left[ \frac{0.15}{8.617 \times 10^{-5}} \times \left( \frac{1}{298} - \frac{1}{T_A + 273} \right) \right] \quad (39)$$

### 4. Simulation Results and Numerical Studies

In this paper, all simulations and calculations were conducted using the MATLAB 2022-b software. To analysis the proposed model for the FC-MCR, the sensitivity of each state in Markov representation to changes in component reliability data is determined in this section. The purpose of this analysis is to prioritize the FC-MCR main components from the effects on availability point of view at various temperatures. In this regard, the numerical data at 27°C are shown in Table 1, and the calculated parameters for the FC-MCR Markov model are presented in Table 2. Since the sensitivity determination of each state in the Markov model shows the effect of input parameters variation on the probability of the occurrence of that state, calculating  $\lambda/\mu$  index for each component allows the possibility of examining the effect of that component on FC-MCR availability. Accordingly, the component with the largest  $\lambda/\mu$  index has the greatest effect on reducing the availability of FC-MCR compared to other components. The results of calculating  $\lambda/\mu$  index for FC-MCR at various operating temperatures are presented in Table 3. As can be seen, FC-MCR availability at 27°C was 0.9943 and in this condition, the MCRCS and WCS had the largest and smallest  $\lambda/\mu$  index compared to other components, respectively. This means that decreasing the failure rate or increasing the repair rate of MCRCS could have the greatest effect on increasing the FC-MCR availability.

#### A) Sensitivity Analysis to components failure and repair rates

In this section, for investigating the effect of each component on FC-MCR availability at 27°C, the effect of component failure and repair rate change on the operating state probability has been examined. In this regard, each component failure and repair rate has been changed independently for

a certain range to specify the effect of component failure and repair rates on the FC-MCR operating state probability. As shown in Figs. 10 and 11, under normal conditions, variation of the MCRCS failure and repair rates will have the greatest effect on the probability of operating states. This fact is also visible in Table 3 showing that under normal conditions, investment in the MCRCS can have the greatest effect on FC-MCR reliability enhancement.

*B) Sensitivity Analysis to Temperature Variations*

In this section, the effect of operating temperature on failure rate and availability of FC-MCR components has been evaluated. As seen in Fig. 12(a), temperature rise led to a relative increase in the failure rate of all FC-MCR components. results presented in Fig. 12 also shows MCRCS at the operating temperatures below 60°C; the ThCS at the operating temperatures ranging from 60°C to 120°C; and the reactor windings at the operating temperatures above 120°C have the greatest variation in failure rate compared to other components. On the other hand, components  $\lambda/\mu$  index variations brought about due to temperature variations in Fig. 12(b) show that at operating temperatures below 45°C, MCRCS has the largest  $\lambda/\mu$  index. Therefore, in this temperature range, MCRCS can have the greatest effect on the FC-MCR availability. However, the operating temperature rise more than 60°C has a significant increase in the windings  $\lambda/\mu$  index in the EMS and then the ThCS in the CMS. Accordingly, when the operating temperature is above 60°C, the reactor windings can have the greatest effect on FC-MCR availability compared to other components. Hence, increasing the repair rate or reducing the failure rate of windings has the greatest effect on increasing the FC-MCR reliability and availability. This fact seen in the numerical results in Table 3 also shows the importance of considering the effect of operating temperature on reliability evaluation and preventive maintenance planning for reactive power sources in power systems.

*C) Comparison of FC-MCR and FC-TCR from Reliability Point of View*

In this section, MCR and TCR-based SVCs are compared from reliability point of view. In this comparison, the three-state Markov model determined in [16] is considered as FC-TCR reliability model. Since FC-TCR cannot directly be connected to the HV network at high voltage levels, its reliability model combines with the three-state Markov model of a power transformer. In reliability modeling of interface transformer, it is assumed that the transformer has a subsystem including active components (windings, core, oil and its tank) and a subsystem including passive components (bushings and winding cooling system).

Table.1.  
The FC-MCR component reliability parameters.

| Components                        | $\lambda$ (f/yr) | $\mu$ (R/yr) |
|-----------------------------------|------------------|--------------|
| MCRCS [16]                        | 0.3121           | 154.75       |
| Thyristor switches [16]           | 0.0361           | 100          |
| ThCS [22]                         | 0.8238           | 100          |
| Core [20]                         | 0.0005           | 19           |
| Oil & Tank [20]                   | 0.0030           | 23           |
| Windings ( $\lambda_{wd}$ ) [20]  | 0.0045           | 100          |
| Windings ( $\lambda_{1wd}$ ) [20] | 0.0030           | -            |
| Windings ( $\lambda_{2wd}$ ) [20] | 0.0450           | -            |
| WCS [20]                          | 0.0010           | 121.67       |
| HV bushings [20]                  | 0.0030           | 182.50       |

Table.2.  
The FC-MCR Markov model failure and repair rates at 27°C.

| Parameters        | Value (occ/yr) | Parameters        | Value (occ/yr) |
|-------------------|----------------|-------------------|----------------|
| $\lambda_{CMS}$   | 0.4907         | $\mu_{EMS}$       | 8.3189         |
| $\mu_{CMS}$       | 129.03         | $\lambda_{MCR}$   | 0.5037         |
| $\lambda_{EMS}$   | 0.0120         | $\lambda_{1-MCR}$ | 0.0002         |
| $\lambda_{1-EMS}$ | 0.0002         | $\lambda_{2-MCR}$ | 0.5432         |
| $\lambda_{2-EMS}$ | 0.0525         | $\mu_{MCR}$       | 95.437         |

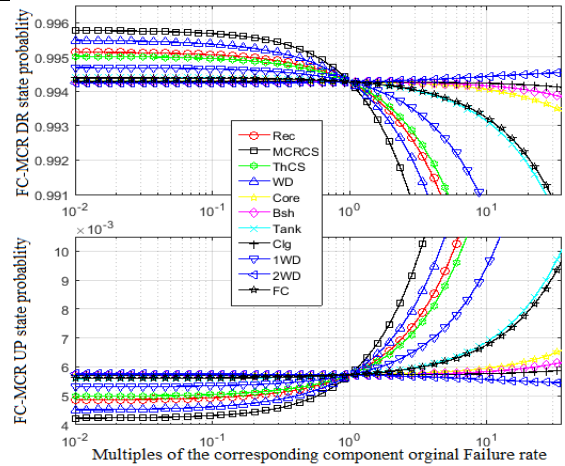


Fig. 10. Effect of components failure rate on FC-MCR Up and DR states probability.

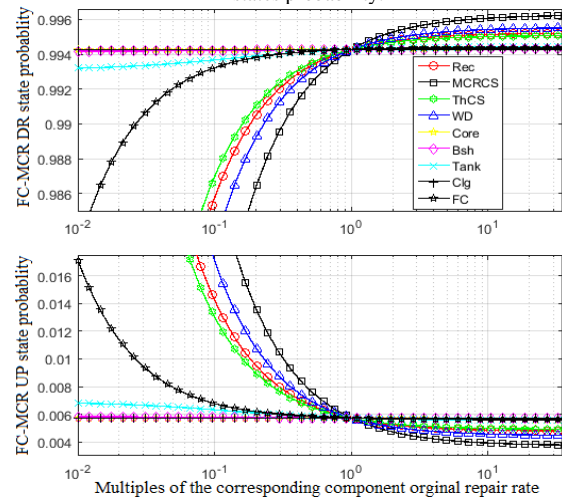


Fig. 11. Effect of components repair rate on FC-MCR Up and DR states probability.

Table 3.  
Numerical results of temperature effect on the FC-MCR reliability indices.

|   |                      | Operating temperatures |           |           |           |           |           |
|---|----------------------|------------------------|-----------|-----------|-----------|-----------|-----------|
|   |                      | 27°C                   | 50°C      | 75°C      | 100°C     | 125°C     | 150°C     |
| FC-MCR $\lambda/\mu$ components indices | FC                   | 0.0001173              | 0.0001774 | 0.0002613 | 0.0003654 | 0.0004898 | 0.0006343 |
|   | MCRCS                | 0.0019908              | 0.0026221 | 0.0033943 | 0.0042445 | 0.0051604 | 0.0061312 |
|   | wd                   | 0.0012328              | 0.0041241 | 0.0153229 | 0.0569315 | 0.2115226 | 0.7859162 |
|   | Rec.                 | 0.0009627              | 0.0014455 | 0.0021221 | 0.0029665 | 0.0039835 | 0.0051736 |
|   | ThCS                 | 0.0008237              | 0.0029873 | 0.0099888 | 0.0284098 | 0.0708588 | 0.1586355 |
|   | Bsh                  | 0.0000164              | 0.0000164 | 0.0000164 | 0.0000274 | 0.0000851 | 0.0001426 |
|   | T&O                  | 0.0001318              | 0.0001318 | 0.0001318 | 0.0002215 | 0.0006829 | 0.0011444 |
|   | Core                 | 0.0000274              | 0.0000274 | 0.0000274 | 0.0000274 | 0.0002741 | 0.0000273 |
|   | WCS                  | 0.0000082              | 0.0000082 | 0.0000082 | 0.0000082 | 0.0000082 | 0.0000082 |
| MCR                                     | UP state probability | 0.9944164              | 0.9879413 | 0.9682716 | 0.9116335 | 0.7669518 | 0.5012869 |
|   | DR state probability | 0.0003688              | 0.0006563 | 0.0010450 | 0.0014308 | 0.0016441 | 0.0013872 |
|   | DN state probability | 0.0052147              | 0.0114023 | 0.0306833 | 0.0869355 | 0.2314070 | 0.4973257 |
| FC-MCR                                  | UP state probability | 0.9942997              | 0.9877660 | 0.9680186 | 0.9113005 | 0.7665763 | 0.5019692 |
|   | DR state probability | 0.0056996              | 0.0122319 | 0.0319733 | 0.0886676 | 0.2333103 | 0.4977155 |
|   | DN state probability | 0.0000006              | 0.0000020 | 0.0000080 | 0.0000317 | 0.0001133 | 0.0003152 |

Combining the FC-TCR and interface transformer Markov models to achieve an SVC equivalent to FC-MCR is shown in Fig. 13. In this Markov representation, the power transformer is considered as one of the SVC main components. Therefore, the maximum compensation capacity is available when all components are healthy, and the failure of the FC-TCR or its interface transformer causes the SVC to be completely removed from service. Accordingly, in the proposed Markov model shown in Fig. 13, State 1 represents the full capacity; states 2, 4, and 5 represent the derated capacity; and states 3, 6, 7, 8, and 9 represent the zero capacity of FC-TCR.

The simulation results presented in Fig. 14 shows the FC-MCR availability at 27°C was 0.9943 which increased significantly compared to FC-TCR availability (0.9688). In addition, the operating temperature rise has shown that FC-MCR will have less sensitivity to temperature variations compared to its counterpart. Determining the numerical values of 0.5019 and 0.3017 for the availability of these two types of SVCs at 150°C shows that in addition to normal operating conditions the use of FC-MCR at higher temperatures can result in higher reliability and availability for the power system compared to FC-TCR. On the other hand, in Fig. 14, the variations in DR and DN states probability show that with a rise in temperature, the probability of occurrence of DR and DN states for FC-MCR is higher and lower than the corresponding values for FC-TCR, respectively. This fact that confirms the superiority of FC-MCR performance at high temperatures, also suggests that failure in FC-MCR components can more likely limit the compensation capacity. Therefore, under similar conditions, FC-TCR components failure probability that causes this

compensator be completely removed from the service is more than the derated state probability.

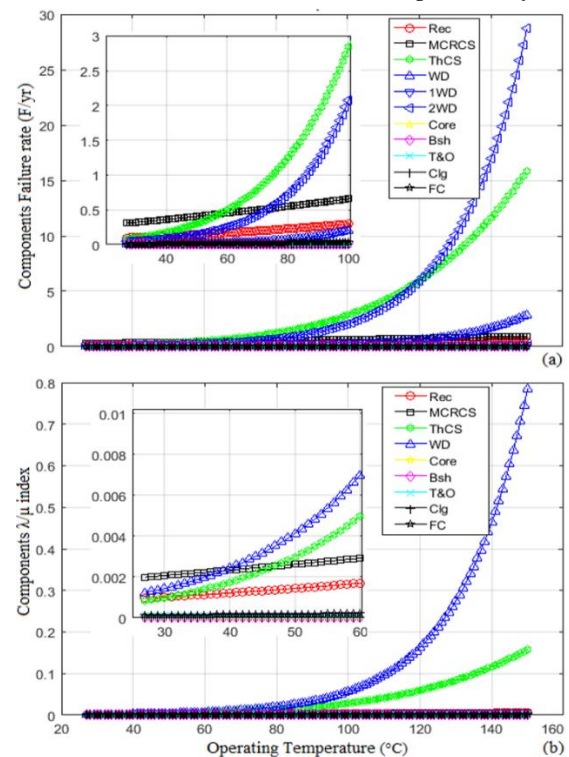


Fig. 12. Effect of operating temperature on components failure rate (a) and  $\lambda/\mu$  index (b).

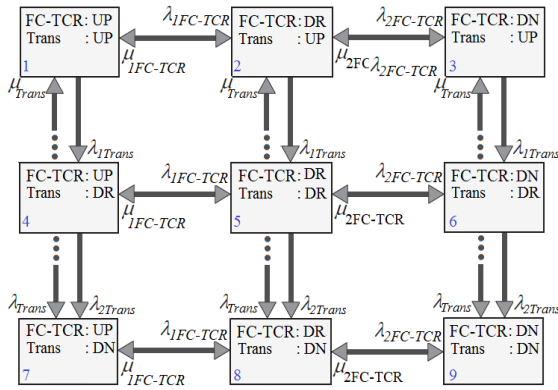


Fig. 13. Proposed Markov model for the FC-TCR and its interface transformer.

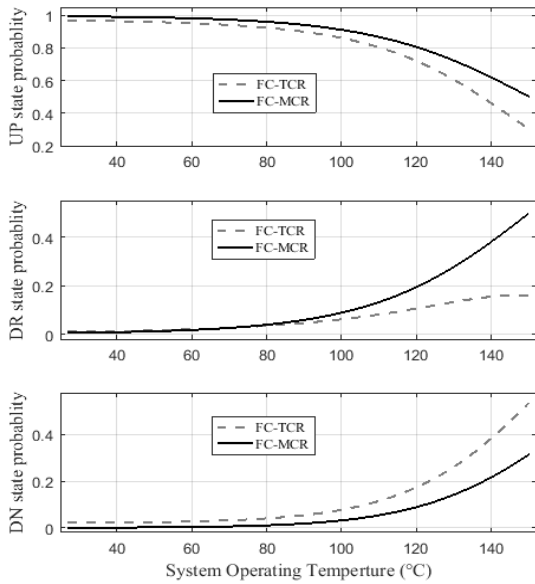


Fig. 14. Performance comparison of TCR- and MCR-based SVCs in various operating conditions.

## 5. Conclusion and Future Direction

This paper proposed a comprehensive model for the reliability evaluation of the FC-MCR using the Markov process approach. In this regard, first, the Markov model of the main components is extracted and next, the extracted models are combined based on the frequency/duration technique. Since thermal management is one of the important aspects in evaluating the electrical equipment reliability in the proposed model, the effect of temperature variations is considered based on the MIL-217F standard with its simulation results presented for various temperatures. The simulation results and sensitivity analysis performed on the variation of Markov model parameters at different temperatures have shown that under various temperature conditions, different components affect the FC-MCR availability. So, measures needed for SVC reliability enhancement can vary at different temperatures.

Future works can be concentrated on applying this model in the reliability evaluation of a test system to consider the effect of SVC operating temperature and reliability parameters on the reliability indices of the whole system. In this paper, only the effect of operating temperature (as the most effective environmental factor) is considered in FC-MCR reliability modeling. Meanwhile, in future works, studying the effect of other environmental factors such as air pressure and relative humidity can bring valuable results in FC-MCR reliability parameters.

## Nomenclature:

|                     |  |
|---------------------|--|
| $\mu_{MCRCS}$       | The repair rate for MCR control system [R/yr]                              |
| $\lambda_{wd}$      | The failure rate of windings from UP to DN [F/yr]                          |
| $\lambda_{1wd}$     | The failure rate of windings from UP to DR [F/yr]                          |
| $\lambda_{2wd}$     | The failure rate of windings from DR to DN [F/yr]                          |
| $\mu_{wd}$          | The repair rate of windings from DN to UP [R/yr]                           |
| $\lambda_{CTO}$     | The equivalent failure rate for CTO set [F/yr]                             |
| $\lambda_{SSi}$     | The failure rate of sub-system $i$ from UP to DN [F/yr]                    |
| $\lambda_{1-SSi}$   | The failure rate of sub-system $i$ from UP to DR [F/yr]                    |
| $\lambda_{2-SSi}$   | The failure rate of sub-system $i$ from DR to DN [F/yr]                    |
| $\mu_{SSi}$         | The repair rate of sub-system $i$ from DN to UP [R/yr]                     |
| $\lambda_{EMS}$     | The failure rate of EMS from UP to DN [F/yr]                               |
| $\lambda_{1-EMS}$   | The failure rate of EMS from UP to DR [F/yr]                               |
| $\lambda_{2-EMS}$   | The failure rate of EMS from DR to DN [F/yr]                               |
| $\mu_{EMS}$         | The repair rate of EMS from DN to UP [R/yr]                                |
| $\lambda_{MCR}$     | The failure rate of MCR from UP to DN [F/yr]                               |
| $\lambda_{1-MCR}$   | The failure rate of MCR from UP to DR [F/yr]                               |
| $\lambda_{2-MCR}$   | The failure rate of MCR from DR to DN [F/yr]                               |
| $\lambda_{b-Th}$    | The failure rate for thyristor switches at 27°C [F/yr]                     |
| $\lambda_{b-MCRCS}$ | The failure rate of MCR control system at 27°C [F/yr]                      |
| $\pi_{T-MCRCS}$     | Temperature factor for MCR control system                                  |
| $\lambda_{1FC-TCR}$ | The failure rate of FC-TCR from UP to DR [F/yr]                            |
| $\lambda_{2FC-TCR}$ | The failure rate of FC-TCR from DR to DN [F/yr]                            |
| $\mu_{2FC-TCR}$     | The repair rate of FC-TCR from DN to DR [R/yr]                             |
| $\mu_{1FC-TCR}$     | The repair rate of FC-TCR from DR to UP [R/yr]                             |
| $\lambda_{Trans}$   | The failure rate of transformer from UP to DN [F/yr]                       |
| $\lambda_{1-Trans}$ | The failure rate of transformer from UP to DR [F/yr]                       |
| $\lambda_{2-Trans}$ | The failure rate of transformer from DR to DN [F/yr]                       |
| $\mu_{Trans}$       | The repair rate of transformer from DN to UP [R/yr]                        |
| $\mu_{MCR}$         | The repair rate of MCR from DN to UP [R/yr]                                |
| $\alpha_B$          | Lifetime characteristics of the pump bearings as a function of temperature |
| $\alpha_w$          | Lifetime characteristics of the pump windings as a function of temperature |
| $\lambda_{CMS}$     | The failure rate for CMS [F/yr]  |
| $\lambda_{ThCS}$    | The failure rate of thyristors cooling [F/yr]                              |
| $\mu_{ThCS}$        | The repair rate of thyristor cooling [R/yr]                                |
| $\mu_{CTO}$         | The equivalent repair rate for CTO set [R/yr]                              |
| $\lambda_{ThCS}$    | The failure rate of thyristors cooling [F/yr]                              |
| $\mu_{ThCS}$        | The repair rate of thyristor cooling [R/yr]                                |
| $\lambda_{T&O}$     | The failure rate of oil and its tank [F/yr]                                |
| $\mu_{T&O}$         | The repair rate of oil and its tank [R/yr]                                 |
| $\lambda_{WCS}$     | The failure rate of windings cooling [F/yr]                                |
| $\mu_{WCS}$         | The repair rate of windings cooling [R/yr]                                 |
| $\lambda_{rec}$     | The failure rate of rectifier [F/yr]                                       |
| $\mu_{rec}$         | The repair rate of rectifier [R/yr]  |
| $\lambda_{core}$    | The failure rate of iron core [F/yr]                                       |
| $\mu_{core}$        | The repair rate of iron core [R/yr]  |
| $\lambda_{Bsh}$     | The failure rate of HV bushings [F/yr]                                     |
| $\mu_{Bsh}$         | The repair rate of HV bushings [R/yr]                                      |
| $\lambda_{b-wd}$    | The failure rate for windings at 27°C [F/yr]                               |
| $\pi_S$             | Electrical stress factor   |
| $\pi_E$             | Environment factor   |
| $\pi_Q$             | The quality factor   |
| $T_A$               | Operating temperature [°C]   |
| $\pi_{T-wd}$        | Temperature factor for windings  |
| $\pi_{T-Bsh}$       | Temperature factor for HV bushings   |
| $\pi_{T-FC}$        | Temperature factor for fixed capacitor (FC)                                |
| $\theta_{ja}$       | Thermal resistance   |
| $P_{loss}$          | Switches losses [W]  |
| $T_{TH}$            | The hot spot temperature [°C]  |
| $P_i$               | The probability of occurrence of state $i$                                 |

|              |   |
|--------------|---|
| $f_{ij}$     | transfer frequency from state $i$ to $j$    |
| $\pi_{T-Th}$ | Temperature factor for thyristor switches   |
| $t$          | The operating time of the circulation pump  |
| $\Delta T$   | Average temperature rise above ambient [°C] |

## References

- [1] L. A. Paredes, M. G. Molina, B. R. Serrano, "Enhancing Dynamic Voltage Stability in Resilient Microgrids Using FACTS Devices," *IEEE Access*, Vol. 11, No. 1, pp. 2169-3536, 2023.
- [2] K. Mehmood, K. M. Cheema, M. F. Tahir, A.I Saleem, A. H. Milyani, "A comprehensive review on magnetically controllable reactor: Modelling, applications and future prospects," *Energy Reports*, Vol. 7, No. 1, pp. 2354-2378, 2021.
- [3] M. Tumaya, T. Demirdelena, S. Balb, R. İ. Kayaalpç, B. Dogruc, M. Aksoyd, "A review of magnetically controlled shunt reactor for power quality improvement with renewable energy applications" *International Journal of Renewable and Sustainable Energy Reviews*, Vol. 77, No. 1, pp. 215–228, 2017.
- [4] T. Zheng, T. Huang, F. Zhang, Y. Zhao, L. Liu, "Modeling and Impacts Analysis of Energization Transient of EHV/UHV Magnetically Controlled Shunt Reactor", *International Transactions on Electrical Energy Systems*, Vol. 27, No. 7, pp. 1-12, 2017.
- [5] B. Shakerighadi, N. Johansson, R. Eriksson, P. Mitra, A. Bolzoni, A. Clark, H. Nee, "An overview of stability challenges for power-electronic-dominated power systems: The grid-forming approach," *IET Generation, Transmission & Distribution*, Vol. 17, No. 2, pp. 284-306, 2023.
- [6] W. Qin, P. Wang, X. Han, X. Du, "Reactive Power Aspects in Reliability Assessment of Power Systems", *IEEE Transaction on Power System*, Vol. 26, No. 1, pp. 85-92, 2011.
- [7] M.A. Nezafat Tabalvandani, M. Hosseini Shirvani, and H. Motameni, "Reliability-aware web service composition with cost minimization perspective: a multi-objective particle swarm optimization model in multi-cloud scenarios," *Soft Computing*, 2023.
- [8] Y. Asghari Alaie, M. Hosseini Shirvani, and A.M. Rahmani, "A hybrid bi-objective scheduling algorithm for execution of scientific workflows on cloud platforms with execution time and reliability approach," *Journal of Supercomputing*, Vol. 79, pp. 1451–1503, 2023.
- [9] R. Billinton, R. N. Allan, "Reliability Evaluation of Power Systems" Plenum Press, NewYork, 1996.
- [10] R. Billinton, W. Li, "Reliability assessment of electric power systems using Monte Carlo methods", Springer Science & Business Media, 2014.
- [11] W. Qin, P. Wang, X. Han, Y. Ding, X. Du, "Reliability Assessment of Power Systems Considering Reactive Power Sources", *IEEE PES General Meeting*, 2009.
- [12] W. Qin, P. Wang, J. Song, Z. Wang, "Reactive power impact on reliability of 220kV Taiyuan Power System", *IEEE 11th Int. Conference on Probabilistic Methods Applied to Power Systems*, pp. 648 – 653, 2010.
- [13] R. Billinton, M. Fotuhi-Firuzabad, S. O. Faried, S. Aboreshaid, "Impact of Unified Power Flow Controllers on Power System Reliability", *IEEE Transaction on Power System*, Vol. 15, No. 1, pp. 410-415, 2000.
- [14] A. H. Etemadi, M. Fotuhi-Firuzabad, "Distribution System Reliability Enhancement Using Optimal Capacitor Placement", *IET Generation, Transmission & Distribution*, Vol. 2, No. 5, pp. 621-631, 2008.
- [15] M. S. Alvarez-Alvarado, D. Jayaweera, "Reliability model for a Static Var Compensator", *IEEE Second Ecuador Technical Chapters Meeting*, 2017.
- [16] A. Karami-Horestani, M. E. Hamedani-Golshan, H. Hajian, "Reliability modeling of TCR–FC type SVC using Markov process", *Electrical Power and Energy Systems*, Vol. 55, No. 1, pp. 305–311, 2014.
- [17] R. R. Karymov, M. Ebadian, "Comparison of Magnetically Controlled Reactor (MCR) and Thyristor Controlled Reactor (TCR) From Harmonics Point of View", *International Journal of Electrical Power & Energy Systems*, Vol. 29, No. 3, pp. 191-198, 2007.
- [18] M. Ebadian, F. Dastyar, "Performance Comparison of Transient Behaviors of Magnetically and Thyristor-Controlled Reactors", *International Journal of Electric Power Components and Systems*, Vol. 38, No. 1, pp. 85-99, 2009.
- [19] M. Chafai, L. Refoufi, H. Bentarzi, "Large Power Transformer Reliability Modeling", *International Journal of System Assurance Engineering and Management*, Vol. 7, No. 1, pp. 9-17, 2016.
- [20] M. Sefidgaran, M. Mirzaie, A. Ebrahimzadeh, "Reliability Model of Power Transformer with ONAF Cooling" *International Journal of Electrical Power and Energy Systems*, Vol. 35, No. 1, pp. 97-104, 2012.
- [21] A. A. Alabduljabbar, CÖ. Gerçek, T. Atalik, et al, "Implementation Aspects and Comprehensive Assessment of a 16 MVAR Static Var Compensator Installed for a Weak Distribution Network", *International Transactions on Electrical Energy Systems*, Vol. 27, No. 8, pp. 1-14, 2017.
- [22] MIL-HDBK-217F, *Military hand-book "Reliability Prediction of Electronic Equipment"*, Department of defense, Washington DC, USA, 1991.
- [23] J. Watson, G. Castro, "High temperature electronics pose design and reliability challenges", *Journal of Analog Dialogue, Analog Devices*, Vol. 46, No. 1, pp. 1-7, 2012.
- [24] V. Lakshminarayanan, N. Sriraam, "The Effect of Temperature on the Reliability of Electronic Components", *IEEE International Conference on Electronics, Computing and Communication Technologies*, 2014.



Morteza Haghshenas received the Ph.D. degree in power electrical engineering from University of Isfahan, Isfahan, Iran, in 2022. He is currently a research assistant with the electrical engineering department, University of Isfahan, Isfahan, Iran. His main area of research interests include: microgrids and active distribution networks, power systems planning and operation, and power system reliability and resiliency studies.



Rahmat-Allah Hooshmand (Senior Member, IEEE) received the Ph.D. degree in electrical engineering from Tarbiat Modarres University, Tehran, Iran, in 1995. He is currently a Professor (Full) with the Electrical Engineering Department, University of Isfahan, Isfahan, Iran. His main area of research interest is modeling of power systems and distribution networks, distributed generation, and power system planning and operation.